

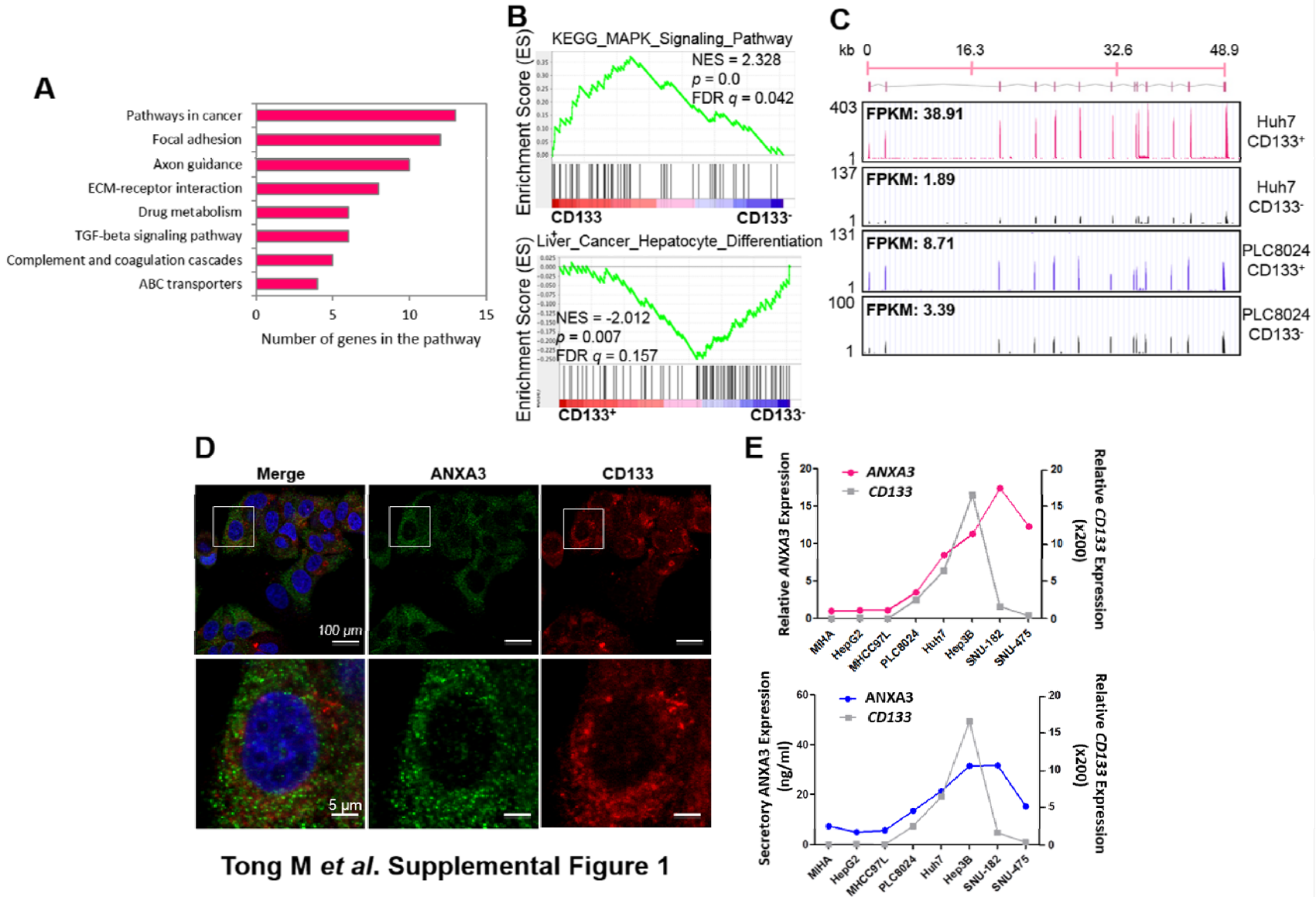
Stem Cell Reports, Volume 5

Supplemental Information

**ANXA3/JNK Signaling Promotes Self-Renewal
and Tumor Growth, and Its Blockade Provides
a Therapeutic Target for Hepatocellular Carcinoma**

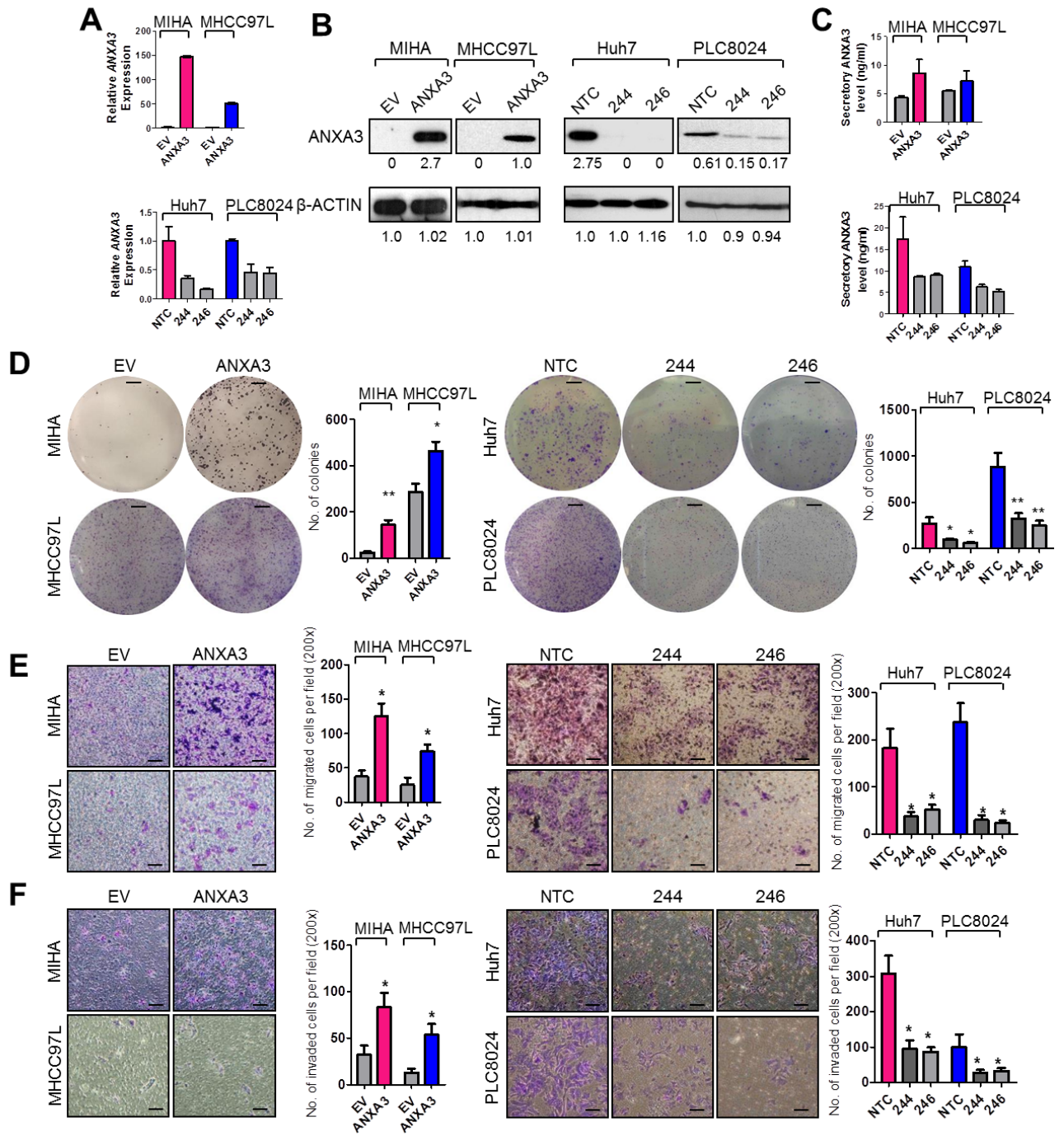
Man Tong, Tsun-Ming Fung, Steve T. Luk, Kai-Yu Ng, Terence K. Lee, Chi-Ho Lin, Judy W. Yam, Kwok Wah Chan, Fai Ng, Bo-Jian Zheng, Yun-Fei Yuan, Dan Xie, Chung-Mau Lo, Kwan Man, Xin-Yuan Guan, and Stephanie Ma

Supplemental Figures and Figure Legends



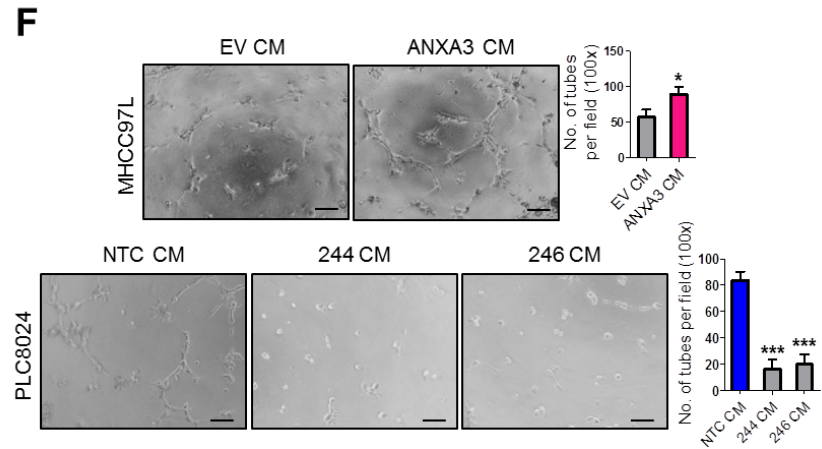
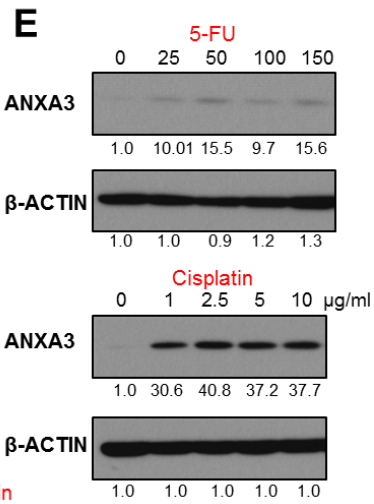
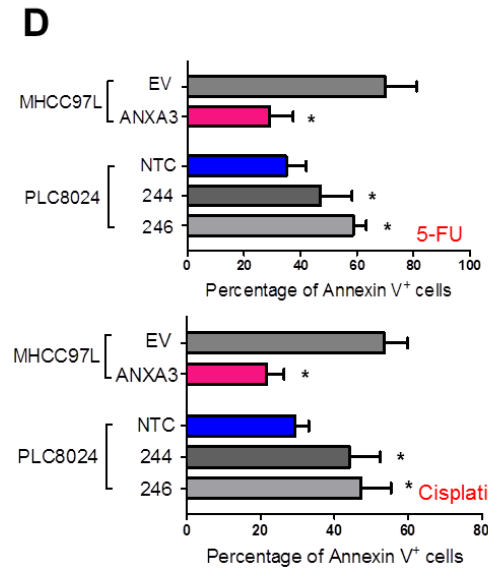
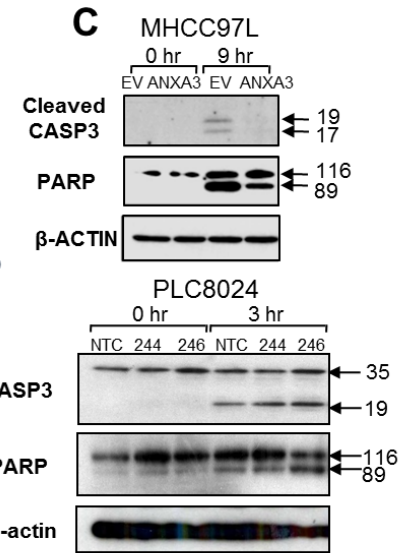
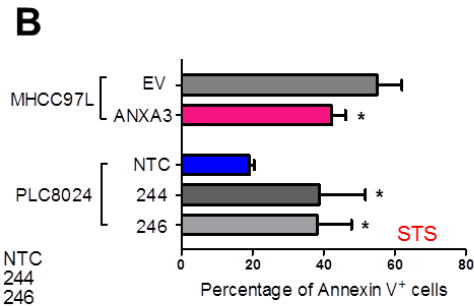
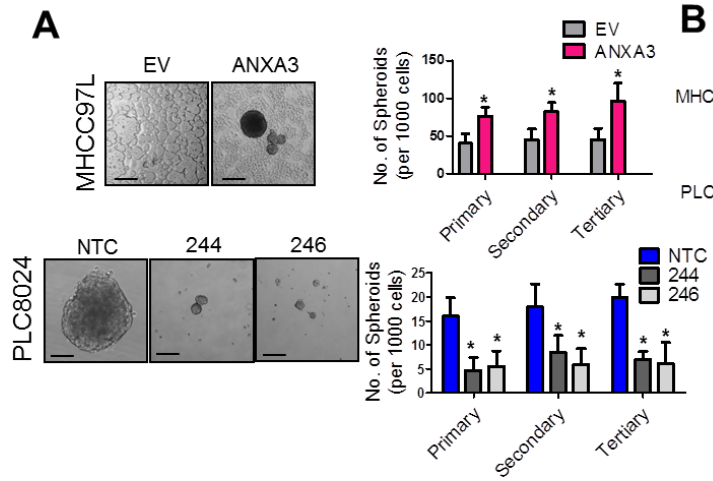
Tong M *et al.* Supplemental Figure 1

Supplemental Figure S1. Positive correlation between ANXA3 and CD133 in HCC. (Related to Figure 1) **(A)** Most significantly enriched pathways common between CD133⁺ liver CSCs vs. CD133⁻ non-CSC subsets isolated from Huh7 and PLC8024 HCC cells by DAVID bioinformatics analysis software. **(B)** GSEA comparison of differentially expressed genes in CD133⁺ vs. CD133⁻ subsets isolated from Huh7 and PLC8024 HCC cells identified enrichment of *MAPK* signaling in CD133⁺ liver CSCs and hepatocyte differentiation in CD133⁻ non-CSC subsets. NES, normalized enrichment score; FDR q , false discovery rate q value. **(C)** RNA-Seq read mapping to the University of California, Santa Cruz (UCSC) reference genome (hg19) of the *ANXA3* (NM_005139) gene. The absolute read counts for each sample are indicated on the y -axis. **(D)** Dual-color IF images of CD133 (red) and ANXA3 (green) in PLC8024 cells. Nuclei stained with DAPI (blue). Images shown of data from 3 independent experiments. **(E)** mRNA and secretory ANXA3 levels across a panel of liver cell lines as detected by qRT-PCR and ELISA, respectively, relative to CD133 expression.



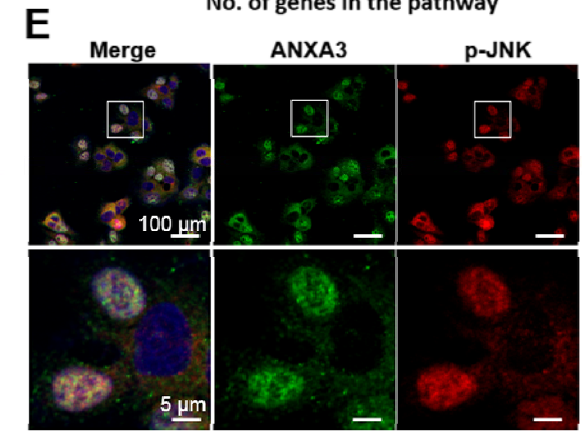
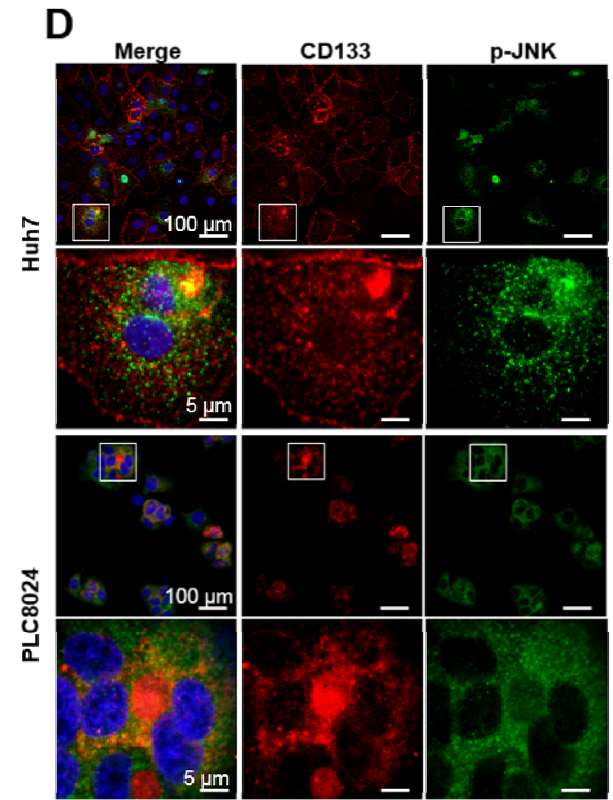
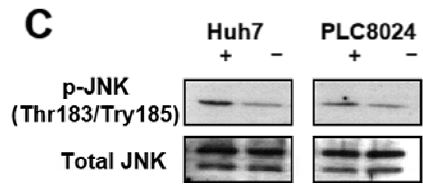
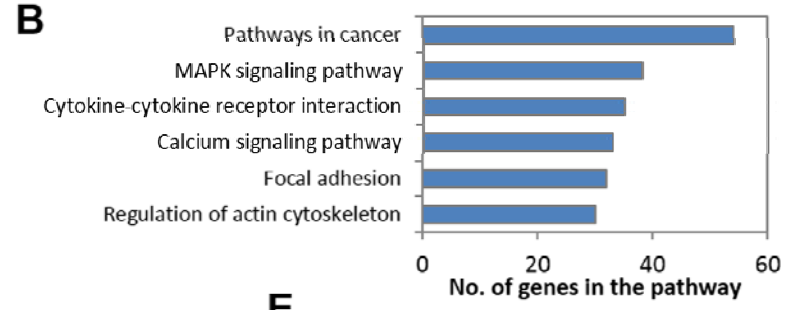
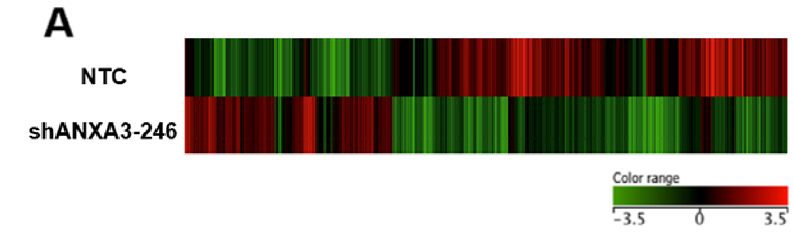
Tong M *et al.* Supplemental Figure 2

Supplemental Figure S2. Endogenous ANXA3 confers enhanced clonogenicity, migration and invasion abilities in HCC. (Related to Figures 2 and 3) **(A to C)** Validation of ANXA3 overexpression (MIHA and MHCC97L) and knockdown (Huh7 and PLC8024) at genomic levels by qPCR, endogenous proteomic levels by Western blot and secretory levels by ELISA. Error bars represent \pm SD. Western blot images shown of data gathered from 3 independent experiments. **(D)** Quantification of colonies induced by the indicated stable cell lines. * p <0.05 and ** p <0.01. Scale 5mm. Results represent mean \pm SD from triplicate wells in 3 independent experiments. **(E and F)** Quantification of number of cells that migrated or invaded in the indicated stable cell lines. * p <0.05. Scale 100 μ m. Results represent mean \pm SD from 3 independent experiments.



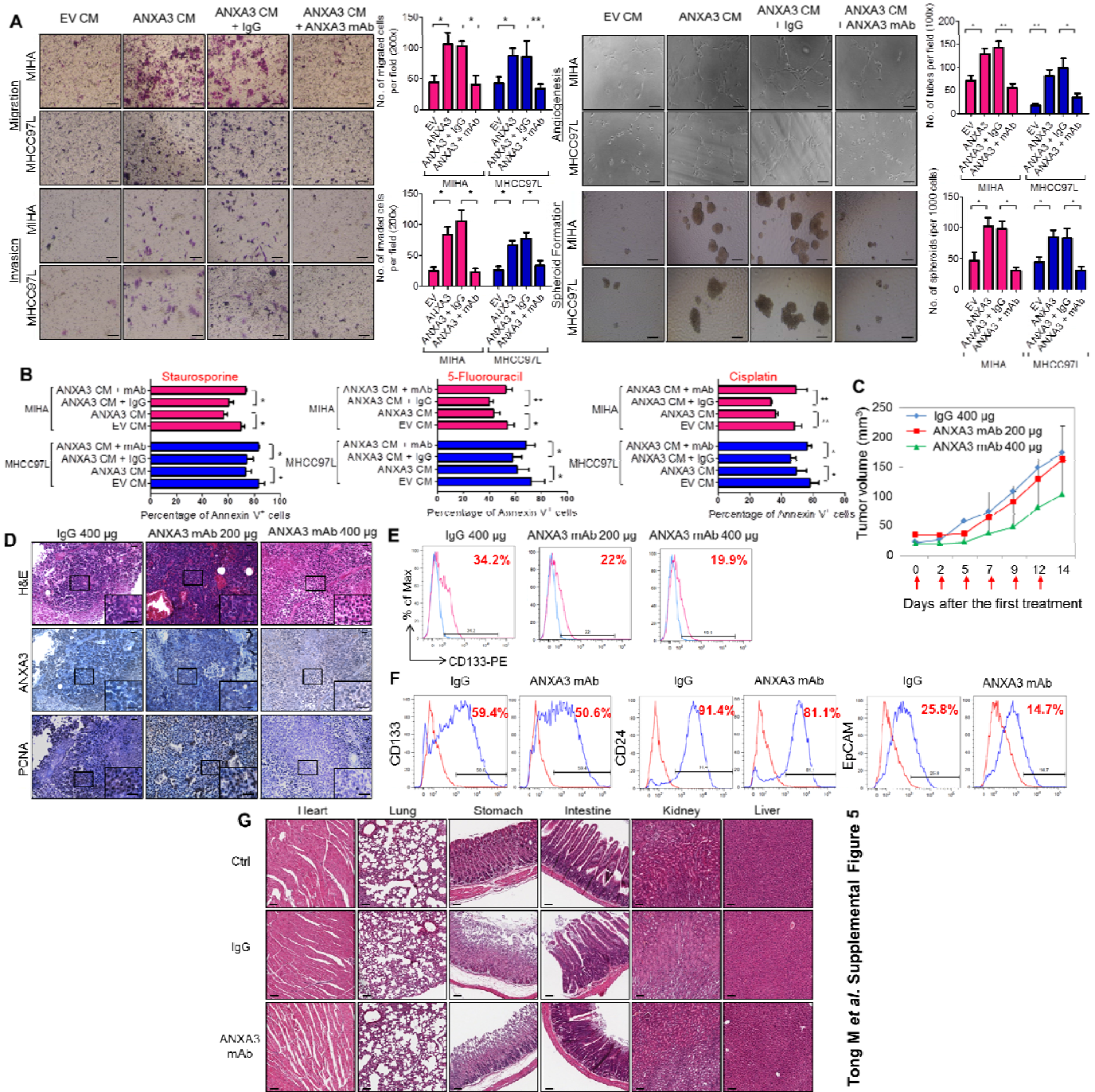
Tong M *et al.* Supplemental Figure 3

Supplemental Figure S3. Endogenous ANXA3 confers enhanced cancer and stem cell-like properties in HCC. (Related to Figures 2 and 3) **(A)** Quantification of primary, secondary and tertiary hepatospheres in HCC cells with ANXA3 stably expressed (MHCC97L EV and ANXA3 O/E) or repressed (PLC8024 NTC and ANXA3 knockdown clones 244 and 246). * $p < 0.05$. Scale 100 μm . Results represent mean \pm SD of 12 replicates in 3 independent experiments. **(B)** Percentage of Annexin V positive cells in MHCC97L and PLC8024 cells with ANXA3 stably expressed and repressed, respectively, following STS treatment. Results represent mean \pm SD of 3 independent experiments. **(C)** Western blot showing expression of total and cleaved forms of caspase 3 and PARP in the indicated stable cell lines after STS treatment for various time points. **(D)** Percentage of Annexin V positive cells in MHCC97L and PLC8024 cells with ANXA3 stably expressed and repressed, respectively, following treatment with chemotherapeutic drugs, 5-FU and cisplatin. Results represent mean \pm SD of 3 independent experiments. **(E)** Western blot showing expression of ANXA3 protein in PLC8024 cells following treatment with increasing concentrations of 5-FU and cisplatin. **(F)** Quantification of capillary tubes formed by HUVEC cells following treatment with supernatant collected from MHCC97L and PLC8024 cells with ANXA3 stably expressed and repressed, respectively. * $p < 0.05$ and *** $p < 0.001$. Scale 100 μm . Results represent mean \pm SD of duplicate wells in 3 independent experiments. Representative images from 3 independent experiments unless otherwise specified.



Tong M *et al.* Supplemental Figure 4

Supplemental Figure S4. ANXA3 and JNK are both preferentially overexpressed in the CD133+ liver CSC subset. (Related to Figure 6) **(A)** Unique gene signatures of PLC8024 HCC cells with or without ANXA3 repressed, as shown by hierarchical cluster analysis (3-fold cutoff). Each cell in the matrix represents a particular expression level of genes, where red and green cells indicate high and low gene expression, respectively. **(B)** Most significantly enriched pathways associated with ANXA3 suppression in HCC by DAVID bioinformatics analysis software. **(C)** Western blot showing expression of p-JNK and total JNK in sorted CD133⁺ and CD133⁻ subsets from Huh7 and PLC8024. Please refer to Figure 1B for CD133, ANXA3 and β -ACTIN expression in CD133 sorted Huh7 and PLC8024. **(D)** Dual-color IF images of CD133 (red) and p-JNK (green) in Huh7 and PLC8024 cells. Nuclei stained with DAPI (blue). **(E)** Dual-color IF images of ANXA3 (green) and p-JNK (red) in PLC8024 cells. Nuclei stained with DAPI (blue). Representative images from 3 independent experiments for all results shown in this Figure.



Supplemental Figure S5. ANXA3 ablation decreases the CD133⁺ liver CSC subpopulation and attenuates tumor formation *in vivo*. (Related to Figure 7) **(A)** Left - Quantification of cells that migrated or invaded following treatment with conditioned medium collected from EV control or ANXA3 overexpressing cells and in the absence or presence of IgG control or ANXA3 monoclonal antibody. Results represent mean \pm SD from 3 independent experiments. Right - Quantification of capillary tubes formed by HUVEC cells and spheroids formed following treatment with conditioned medium collected from EV control or ANXA3 overexpressing cells and in the absence or presence of IgG control or ANXA3 monoclonal antibody. * p <0.05 and ** p <0.01. Scale 100 μ m. Results represent mean \pm SD of duplicate wells in 3 independent experiments. **(B)** Percentage of Annexin V positive cells in MIHA and MHCC97L cells following treatment with conditioned medium collected from EV control or ANXA3 overexpressing cells and in the absence or presence of IgG control or ANXA3 monoclonal antibody. * p <0.05 and ** p <0.01. Results represent mean \pm SD of 3 independent experiments. **(C)** Graph showing the average tumor volumes of mice in each group along the course of treatment. Red arrows indicate the days when treatment was administered. Results represent mean \pm SD of 5 mice from 1 independent experiment. **(D)** H&E images and IHC staining for expression of ANXA3 and PCNA in the resected xenograft tumors derived from the indicated treatment groups. Scale 200 μ m. **(E)** Flow cytometry analysis for expression of CD133 in the residual xenografts of the indicated treatment groups. **(F)** Flow cytometry analysis for expression of CD133, CD24 and EpCAM in Huh7 cells treated with IgG control or ANXA3 monoclonal antibody *in vitro*. **(G)** H&E images of major organs (heart, lung, stomach, intestine, kidney and liver) harvested from control untreated mice and mice treated with either IgG control or ANXA3 monoclonal antibody. Scale 100 μ m. Representative images from 3 independent experiments unless otherwise specified.

Supplemental Tables

Supplemental Table S1. Summary of RNA-Seq statistics and mapped reads for sorted CD133⁺ and CD133⁻ cells isolated from Huh7 and PLC8024. (Related to Figure 1)

Sample ID	No. of raw reads	No. of reads after filtering ¹	% of filtered reads	No. of reads mapped to reference genome ²	% of mappable reads ³
Huh7 CD133 ⁺	65,441,262	62,913,906	96.14%	60,149,975	95.61%
Huh7 CD133 ⁻	70,077,984	66,584,108	95.01%	63,376,438	95.18%
PLC8024 CD133 ⁺	63,294,766	60,749,226	95.98%	58,238,955	95.87%
PLC8024 CD133 ⁻	66,357,576	63,563,976	95.79%	60,878,505	95.78%
Average	66,292,897	63,452,804	95.73%	60,660,968	95.61%

¹Raw reads were filtered with polymer track, adaptor sequences and rRNA repeating sequences.

²Sequencing reads were mapped to NCBI Build 37.1 (Genome Reference Consortium GRCh37 / hg19) with at most 2 mismatches.

³Percentage of mappable reads are the percentages of total filtered reads mapped to reference genome.

Supplemental Table S2. List of commonly differentially expressed genes in Huh7 and PLC8024 CD133⁺ vs. CD133⁻ identified by RNA-Seq profiling. *p* < 0.05. (Related to Figure 1)

Gene ¹	Huh7 CD133 ⁺ FPKM	Huh7 CD133 ⁻ FPKM	Huh7 fold- change	PLC8024 CD133 ⁺ FPKM	PLC8024 CD133 ⁻ FPKM	PLC8024 fold-change
Up-regulated genes in the CD133⁺ subset						
<i>PROM1</i>	71.24	1.76	40.40	31.01	5.75	5.39
<i>ANXA3</i>	38.91	1.89	20.60	8.71	3.39	2.57
<i>CFTR</i>	1.50	0.09	17.20	3.15	0.67	4.72
<i>LRP2</i>	13.17	0.78	16.81	11.00	4.01	2.75
<i>BCO2</i>	1.93	0.16	12.44	0.21	0.07	3.07
<i>CCNJL</i>	5.25	0.43	12.32	17.06	7.34	2.32
<i>EDN1</i>	3.11	0.26	12.14	3.11	0.60	5.14
<i>ANKRD1</i>	12.67	1.23	10.31	3.17	0.66	4.79
<i>IL18</i>	24.39	2.42	10.08	16.72	7.96	2.10
<i>MTRNR2L6</i>	8.78	1.00	8.81	8.25	2.83	2.91
<i>THSD4</i>	1.81	0.21	8.44	0.08	0.03	2.77
<i>FSTL1</i>	2.59	0.35	7.47	0.50	0.21	2.34
<i>PRSS23</i>	6.77	0.91	7.43	14.39	2.61	5.52
<i>VIM</i>	128.35	20.82	6.17	19.20	4.98	3.86
<i>UBASH3B</i>	0.96	0.18	5.45	7.84	2.41	3.25
<i>DPP4</i>	100.72	18.55	5.43	0.06	0.03	2.21
<i>MOXD1</i>	1.75	0.32	5.41	3.41	0.65	5.21
<i>MTRNR2L10</i>	3.39	0.65	5.23	3.98	0.56	7.08
<i>SULT1E1</i>	17.79	3.49	5.09	0.06	0.02	3.85
<i>CTTNBP2</i>	2.06	0.44	4.70	0.19	0.02	8.59
<i>AOX1</i>	4.73	1.01	4.69	0.06	0.01	10.38
<i>TFPI2</i>	14.70	3.14	4.68	9.16	4.32	2.12
<i>CYR61</i>	7.32	2.24	3.27	30.80	6.42	4.80
<i>DNAH5</i>	0.04	0.02	2.35	0.47	0.09	4.95
<i>KCP</i>	0.67	0.29	2.35	0.04	0.01	3.22
<i>GJA1</i>	149.41	65.00	2.30	100.28	14.13	7.10
<i>THBS1</i>	2.89	1.27	2.27	9.90	1.75	5.64
<i>PGBD5</i>	1.39	0.63	2.20	7.50	2.26	3.32
<i>TMEM200A</i>	2.93	1.36	2.16	1.94	0.41	4.73
<i>SLC2A3</i>	1.24	0.61	2.05	123.22	42.98	2.87
<i>CDH2</i>	45.28	22.36	2.03	0.56	0.08	6.81
Down-regulated genes in the CD133⁺ subset						
<i>ORM1</i>	114.56	248.10	0.46	75.10	238.49	0.31
<i>ORM2</i>	56.88	125.16	0.45	21.10	63.62	0.33
<i>AHSG</i>	69.28	174.14	0.40	1.12	3.99	0.28
<i>HAL</i>	2.53	6.79	0.37	2.27	9.89	0.23
<i>F5</i>	2.56	10.25	0.25	1.32	2.71	0.49
<i>PCSK9</i>	5.97	25.16	0.24	16.23	43.57	0.37
<i>NKX3-1</i>	0.38	2.94	0.13	0.05	0.14	0.36

¹Genes that encode for secretory proteins are denoted in red italics and in bold font.

Supplemental Table S3. Clinico-pathological correlation of endogenous ANXA3 expression in 83 HCC tissue samples. (Related to Figure 1)

Clinical Features	Total no. of cases ¹	Without ANXA3 overexpression ²	ANXA3 overexpression ²	p value
Gender				
Male	67	33 (49.3%)	34 (50.7%)	0.856
Female	15	7 (46.7%)	8 (53.3%)	
Age				
<50	45	19 (42.2%)	26 (57.8%)	0.19
≥50	37	21 (56.8%)	16 (43.2%)	
HBsAg				
Negative	9	3 (33.3%)	6 (66.7%)	0.288
Positive	71	37 (52.1%)	34 (47.9%)	
HCV antibody				
Negative	79	40 (50.6%)	39 (49.4%)	1
Positive	1	0 (0%)	1 (100%)	
Cirrhosis				
No / Mild	56	24 (42.9%)	32 (57.1%)	0.071
Moderate / Severe	23	15 (65.2%)	8 (34.8%)	
No. of nodules				
Single	68	35 (51.5%)	33 (48.5%)	0.39
Multiple	13	5 (38.5%)	8 (61.5%)	
Tumor size				
<5 cm	76	38 (50%)	38 (50%)	1
≥5 cm	5	2 (40%)	3 (60%)	
Vascular invasion				
Negative	71	37 (52.1%)	34 (47.9%)	0.312
Positive	10	3 (30%)	7 (70%)	
Encapsulation				
No / Incomplete	46	21 (45.7%)	25 (54.3%)	0.441
Complete	35	19 (54.3%)	16 (45.7%)	
Adjacent organ invasion				
Negative	70	34 (48.6%)	36 (51.4%)	0.927
Positive	12	6 (50%)	6 (50%)	
HCC stage				
Stage I / II	60	34 (56.7%)	26 (43.3%)	*0.027
Stage III	21	6 (28.6%)	15 (71.4%)	
Differentiation				
Poor	38	17 (44.7%)	21 (55.3%)	0.263
Moderate	35	17 (48.6%)	18 (51.4%)	
Well	6	5 (83.3%)	1 (16.6%)	
Satellite				
Negative	56	26 (46.4%)	30 (53.6%)	0.473
Positive	14	8 (57.1%)	6 (42.9%)	

¹Clinical data was not available for some patients; statistics were calculated based on available data only.

²HCC specimens demonstrating a fold-change increase of over 1.5 as compared to matched non-tumor samples are classified as ANXA3 overexpression.

Supplemental Table S4. Clinico-pathological correlation of secretory ANXA3 levels in 60 HCC serum samples. (Related to Figure 1)

Clinical Features	Total no. of cases ¹	Low ANXA3 ²	High ANXA3 ²	p value
Gender				
Male	48	19 (39.6%)	29 (60.4%)	*0.011
Female	11	9 (81.8%)	2 (18.2%)	
Age				
<59	29	16 (55.2%)	13 (44.8%)	0.243
≥59	30	12 (40.0%)	18 (60%)	
Family history				
Negative	50	21 (42.0%)	29 (58.0%)	0.071
Positive	9	7 (77.8%)	2 (22.2%)	
AFP elevation				
Negative	45	19 (42.2%)	26 (57.8%)	0.149
Positive	14	9 (64.3%)	5 (35.7%)	
HBeAg				
Negative	31	20 (64.5%)	11 (35.5%)	0.111
Positive	13	5 (38.5%)	8 (61.5%)	
HbsAg				
Negative	51	25 (49%)	26 (51%)	1
Positive	7	3 (42.9%)	4 (57.1%)	
HCV carrier				
Negative	57	27 (47.4%)	30 (52.6%)	1
Positive	2	1 (50%)	1 (50%)	
No. of nodules				
Single	29	18 (62.1%)	11 (37.9%)	*0.036
Multiple	29	10 (34.5%)	19 (65.5%)	
Tumor size				
<5 cm	49	27 (55.1%)	22 (44.9%)	*0.005
≥5 cm	8	0 (0%)	8 (100%)	
HCC stage				
Stage I / II	29	21 (72.4%)	8 (27.6%)	*<0.001
Stage III / VI	30	7 (23.3%)	23 (76.7%)	
Previous malignancy				
Negative	55	28 (50.9%)	27 (49.1%)	0.114
Positive	4	0 (0%)	4 (100%)	

¹Clinical data was not available for some patients; statistics were calculated based on available data only.

²HCC serum samples are classified into low / high ANXA3 based on the median serum ANXA3 level among all cases.

Supplemental Experimental Procedures

Cell lines. Human HCC cell lines, Hep3B, SNU-182, SNU-475 and HepG2, were purchased from American Type Culture Collect (ATCC). HCC cell line, PLC8024, was obtained from the Institute of Virology, Chinese Academy of Medical Sciences, Beijing, China. HCC cell line, Huh7, was provided by Dr. H. Nakabayashi, Hokkaido University School of Medicine, Japan. Immortalized normal liver cell line, MIHA, was provided by Dr. J. R. Chowdhury, Albert Einstein College of Medicine, New York. Metastatic human HCC cell line, MHCC97L, was obtained from the Liver Cancer Institute, Fudan University, Shanghai, China. Chinese hamster ovary cell line CHO-K1 was purchased from ATCC. 293FT cells used for lentiviral transduction and human umbilical vein endothelial cells (HUVEC) were purchased from Invitrogen. All cell lines used in this study were regularly authenticated by morphological observation and tested for absence of Mycoplasma contamination (MycoAlert, Lonza).

Patient samples. Primary human HCC and adjacent non-tumor liver tissue samples were obtained from 83 patients undergoing surgical resection at either the Queen Mary Hospital in Hong Kong or the Sun Yat-Sen University Cancer Centre in Guangzhou, China. Venous blood samples were collected from 60 HCC patients, 20 HBV carriers, 20 patients with liver cirrhosis and 32 normal control individuals. Tissue samples were collected from patients who had not received any previous local or systemic treatment prior to operation. Venous blood samples were collected from HCC patients before any therapeutic procedures were performed. Use of human samples was approved by the committee for ethical review of research involving human subjects at the Queen Mary Hospital or Sun Yat-Sen University Cancer Centre.

Reagents, kits and plasmids. Serum ANXA3 and secretory ANXA3 in conditioned media was quantified using the Human ANXA3 ELISA Kit (Cusabio Biotech). Serum AFP was quantified using the AFP ELISA kit (Aviva Systems Biology). The human recombinant ANXA3 protein used for functional studies was purchased from Origene. JNK inhibitor SP600125 was purchased from Calbiochem. JNK activity was determined by KinaseSTAR™ JNK Activity Assay Kit (BioVision). A FLAG-tagged ANXA3 sequence was cloned into pcDNA6B/myc-His B vector (Invitrogen) in between EcoRI and XhoI or into pSNAP-tag (T7)-2 vector (New England Biolabs) in between EcoRI and HindIII.

Flow cytometry and cell sorting. Flow cytometry analysis or flow cytometry cell sorting was conducted using PE-conjugated mouse anti-human CD133 (Miltenyi Biotec), PE-conjugated mouse anti-human CD24, FITC-conjugated mouse anti-human EpCAM (BD Biosciences) or their respective

isotype controls. Samples were analyzed and sorted on BD FACSCanto II and FACSARIA I, respectively (BD Biosciences) with data analyzed by FlowJo (Tree Star Inc.). For analysis and cell sorting of freshly resected clinical samples and xenograft tumors, tissue samples would first be digested with a mixture of Liberase, DNase I (Roche) and complete DMEM/F12 medium (Invitrogen) on a Miltenyi Biotec gentleMACS dissociator (Miltenyi Biotec), passed through 100 μ M strainers with single cells stained with 7-AAD (BD Biosciences) to exclude dead cells. Detailed protocols described in our previous studies (Ma et al., 2010; Tang et al., 2012).

RNA sequencing. RNA sequencing was performed as a service at the Centre for Genomic Sciences of The University of Hong Kong. Expression levels were tabulated in accordance with the number of exon reads to the length of exons within that gene and per million mapped reads (FPKM).

Quantitative real-time PCR. Total RNA was extracted using RNA-IsoPlus (Takara) and cDNA was synthesized by PrimeScript RT Master Mix (Takara). qPCR was performed with SYBR Green PCR Master Mix (Applied Biosystems) and the following primers *ANXA3*: F (5'-GCAGGAGGAAGGGGTGCGGT-3'); R (5'-TCCAAAGCGCGGTGGGGGAA-3') and *β -ACTIN*: F (5'-CATCCACGAACTACCTTCAACTCC-3'); R (5'-GAGCCGCCGATCCACACG-3') on an ABI Prism 7900 System (Applied Biosystems) with data analyzed using the ABI SDS v2.3 software (Applied Biosystems). Relative expression differences were calculated using the $2^{-\Delta\Delta C_t}$ method.

Western blot and immunoprecipitation. Protein lysates were quantified and resolved on a SDS-PAGE gel, transferred onto a PVDF membrane (Millipore) and immunoblotted with a primary antibody, followed by incubation with a secondary antibody. Antibody signal was detected using an enhanced chemiluminescence system (GE Healthcare). The following antibodies were used: ANXA3 (1:800, Abcam, ab33068), CD133 (1:800, Miltenyi Biotec, 130-092-395), CAV1 (1:5000, BD Biosciences, 610060), caspase 3 (1:1000, Cell Signaling Technology, 9662), PARP (1:1000, Cell Signaling Technology, 9542), p-JNK1 (Thr183/Tyr185) (1:2000, Cell Signaling Technology, 9255), total JNK (1:1000, Cell Signaling Technology, 9252), p-MKK4 (Ser257/Thr261) (1:1000, Cell Signaling Technology, 9156), C-MYC (1:500, Invitrogen, 13-2500), p21 (1:1000, Cell Signaling Technology, 2946), FLAG (1:5000, Sigma-Aldrich, F3165), β -ACTIN (1:5000, Sigma-Aldrich, A5316) and GAPDH (1:1000, Cell Signaling Technology, 5174). Immunoprecipitation was performed with anti-FLAG M2 affinity gel (Sigma-Aldrich). ImageJ software was used for densitometric analyses of western blot bands, and the quantification results were normalized to the loading control.

Luciferase reporter assay. A luciferase reporter construct consisting of the consensus sequence of AP-1 binding site was co-transfected with a Renilla luciferase reporter construct into cells plated on 96-well using Lipofectamine 2000 (Invitrogen). 48 hours after transfection, reporter activity was determined using the Dual-Glo Luciferase Assay Kit (Promega) according to the manufacturer's protocol and measured with plate reader (Victor³ 1420 Multilabel Plate Counter) (Perkin Elmer). Experiments were performed in triplicates.

Lentiviral transduction. ANXA3-specific shRNA expression vectors (NM_0005139), CAV1-specific shRNA expression vectors (NM_001753) and the scrambled shRNA non-target control (NTC) were purchased from Sigma-Aldrich. Sequences of the two shRNAs directed against ANXA3 are as follows: clone ID TRCN0000056244 (CCGGCCAGATCAGAAATTGACCTTTCTCGAGAAAGGTCAATTTCTGATCTGGTTTTTG) and clone ID TRCN0000056246 (CCGGGTAAGAGATTATCCAGACTTTCTCGAGAAAGTCTGGATAATCTCTTACTTTTTG). Sequences of the two shRNAs directed against CAV1 are as follows: clone ID TRCN0000008001 (CCGGGACCCTAAACACCTCAACGATCTCGAGATCGTTGAGGTGTTTAGGGTCTTTTT) and clone ID TRCN0000008002 (CCGGGACGTGGTCAAGATTGACTTTCTCGAGAAAGTCAATCTTGACCACGTCTTTTT). Sequence of NTC is (CCGGCAACAAGATGAAGAGCACAACCTCGAGTTGGTGCTTTCATCTTGTGTTTTT). Sequences were transfected into 293FT cells and packaged using MISSION Lentiviral Packaging Mix (Sigma-Aldrich). ANXA3 lentiviral overexpression or empty vector control plasmids were purchased from GeneCopoeia. CAV1 open reading frame sequence was cloned into pLenti6/V5-D-TOPO-Myc vector. Sequences were transfected into 293FT cells and packaged using Lenti-Pac HIV expression packaging mix (GeneCopoeia) or Viral Power packaging mix (Invitrogen). Virus-containing supernatants were collected for subsequent transduction to establish cells with ANXA3 or CAV1 stably repressed or overexpressed. Puromycin and blasticidin were used to select for cells with stable overexpression of ANXA3 and CAV1, respectively.

Immunohistochemistry. Slides were heated for antigen retrieval in 10 mM sodium citrate (pH 6.0). Endogenous peroxidase activity was inhibited with 3% hydrogen peroxide. Sections were subsequently incubated with mouse anti-human PCNA (Santa Cruz) or mouse anti-human ANXA3 (Origene). Reaction was developed with DAB+ Substrate-Chromogen System (Dako). Slides were counterstained with Mayer's hematoxylin.

Immunofluorescence and confocal microscopy. Cells were fixed with 4% paraformaldehyde, permeabilized with 0.1% Triton X (Sigma), blocked with normal goat serum and incubated with PE-

conjugated mouse anti-human CD133 (Miltenyi Biotec), rabbit anti-human ANXA3 or rabbit anti-human phospho-JNK (Thr183/Tyr185) (Cell Signaling Technology), followed by Alexa-Fluor conjugated secondary antibody, where appropriate. Cells were counterstained with anti-fade DAPI (Invitrogen) and visualized by fluorescent confocal microscope (Carl Zeiss LSM 700). For confocal imaging analysis of ANXA3 internalization, cells were labeled with Vybrant CFDA SE Cell Tracer Kit (Invitrogen). SNAP-tagged ANXA3 proteins labeled with SNAP-Surface Alexa Fluor 546 substrate (New England Biolabs) were co-cultured with CFDA-dye labeled cells for 3 hours. Cells were fixed with 1% paraformaldehyde and visualized by fluorescent confocal microscope (Perkin Elmer).

Hepatosphere-forming and self-renewal assay. Single cells were cultured in 300 μ l of serum-free DMEM/F12 medium (Invitrogen) supplemented with 20 ng/ml human recombinant epidermal growth factor (Sigma-Aldrich), 10 ng/ml human recombinant basic fibroblast growth factor (Sigma-Aldrich), 4 μ g/ml insulin (Sigma-Aldrich), B27 (1:50; Invitrogen), 500 U/ml penicillin, 500 μ g/ml streptomycin (Invitrogen) and 1% methylcellulose (Sigma-Aldrich). Cells were cultured in suspension in poly-HEMA-coated 24-well plates. Cells were replenished with 30 μ l of supplemented medium every second day. To propagate spheres *in vitro*, spheres were collected by gentle centrifugation and dissociated to single cells using TrypLE Express (Invitrogen). Following dissociation, trypsin inhibitor (Invitrogen) was used to neutralize the reaction, and the cells were cultured to generate the next generation of spheres.

Colony formation assay. 1×10^3 cells were seeded in a 6-well plate and cultured in complete medium for 2 weeks. Surviving colonies (>50 cells per colony) were counted and stained with crystal violet (Sigma-Aldrich).

Cell motility and invasion assays. Migration and invasion assays were conducted in 24-well Millicell hanging inserts (Millipore) and 24-well BioCoat Matrigel Invasion Chambers (BD Biosciences), respectively. Cells re-suspended in serum free DMEM were added to the top chamber and medium supplemented with 10% FBS was added to the bottom chamber as a chemoattractant. After 48 hrs of incubation at 37°C, cells that migrated or invaded through the membrane (migration) or Matrigel (invasion) were fixed and stained with crystal violet (Sigma-Aldrich). The number of cells was counted in 3 random fields under 20x objective lens and imaged using SPOT imaging software (Nikon).

Annexin V apoptosis assay. Cells were treated with either 1 μ g/mL STS for 6-16 hrs or with various concentrations of chemotherapeutic drugs, 5-FU and cisplatin (Huh7 with 150 mg/mL 5-FU or 1

mg/mL cisplatin and PLC8024 with 75 mg/mL 5-FU or 2 mg/mL cisplatin) for 48 hrs. Following treatment, cells were harvested and stained with propidium iodide (PI) and FITC-conjugated Annexin V as provided by the Annexin V-FLUOS Staining Kit (Roche). Samples were analyzed on BD FACSCanto II (BD Biosciences) with data analyzed by FlowJo (Tree Star Inc.).

Capillary tube formation assay in HUVECs. Cells were cultured in 6-well plates in complete medium, with culture medium replaced with serum free medium after 24 hrs. Conditioned medium was collected and filtered after incubation for a further 24 hrs. HUVECs were co-cultured with conditioned medium for 24 hrs. Capillary tube formation assays were then conducted on BD Matrigel Basement Membrane Matrix (BD Biosciences). The number of capillary tubes formed was counted in 3 random fields under a 20x objective lens and imaged using SPOT imaging software. Specifically, the formation of 1 capillary tube was defined as a connection between 2 cells.

Animal studies. The study protocol was approved by and performed in accordance with the Committee of the Use of Live Animals in Teaching and Research at The University of Hong Kong. Tumorigenicity was determined by subcutaneous injection into the flank of 4-to-5 week old male BALB/C nude or NOD/SCID mice. Tumor-initiating and self-renewal abilities were investigated by limiting dilution and serial transplantation assays. 4-to-6 week old male NOD/SCID mice were injected subcutaneously with either 5,000 or 10,000 cells. Tumor incidence and tumor latency were recorded. Established xenografts were harvested and dissociated for subsequence passage to secondary mouse recipients. After tumors were detected, tumor sizes were measured every 3 days by calipers and tumor volumes were calculated as $\text{volume (cm}^3\text{)} = L \times W^2 \times 0.5$ with L and W representing the largest and smallest diameters, respectively. Tumors formed were harvested for histological analysis. Metastasis was assessed by orthotopically injecting into the liver of 6 week old BALB/C nude mice to observe for lung metastasis. Specifically, luciferase-labeled cells were injected into the left lobes of the livers of BALB/C nude mice. Six weeks after implantation, mice were administered with 100 mg/kg D-luciferin via peritoneal injection 5 mins before bioluminescent imaging (IVIS™ 100 Imaging System, Xenogen). Livers were harvested for ex-vivo imaging and histological analysis. Animals that were injected with tumor cells but showed no sign of tumor burden were generally terminated six months after tumor cell inoculation, and animals were opened up at the injection sites to confirm that there was no tumor development.

Microarray expression analysis. RNA was assayed on the Affymetrix microarray platform with the Human Genome U133 Plus 2.0 GeneChips and analyzed using MicroArray Suite 5 (MAS5) method with

GeneSpring GX v.12 (Agilent). Experiments were carried out as a service at the Centre for Genomic Sciences of The University of Hong Kong. Pathway enrichment analyses on the differentially expressed genes were conducted using the web resource from The Database for Annotation, Visualization and Integrated Discovery (DAVID) version 6.7 (NIH) and GeneGo Metacore (Thomson Reuters).

ANXA3 monoclonal antibody production. Mouse anti-human ANXA3 monoclonal antibody (that recognizes the epitope peptides ENRWGTDEDK) was synthesized by AbMart, Shanghai, China.

Statistical analysis. Statistical analyses were performed using GraphPad Prism 5.0 (GraphPad Software, Inc.) and SPSS version 21.0 (IBM). Independent Student's *t*-test was used to compare the mean value of two groups. Clinico-pathological significance in clinical samples was evaluated by Fisher's exact test and independent Student's *t*-test for categorical data and continuous data, respectively. ROC analysis was performed using ROC-kit (GUI version 1.0.1, ROC libraries 1.0.3) developed by The University of Chicago. Statistical significance was defined as $p \leq 0.05$.